

**Investigation of 304L stainless steel in a NaCl solution using a microcapillary
electrochemical droplet cell: Comparison with conventional electrochemical techniques**

Farzin Arjmand and Annemie Adriaens^{1,*}

Department of Analytical Chemistry, Ghent University, Krijgslaan 281-S12, 9000 Ghent,
Belgium

* To whom correspondence should be addressed.

Email address: annemie.adriaens@ugent.be; Tel +32 9 264 4826, Fax: +32 9 264 4960

Abstract

In this work a comparison has been made between a localized (micro scale) and a conventional (large scale) corrosion study of 304L stainless steel in a sodium chloride solution using Tafel plots and electrochemical impedance spectra. Results show the high ability of microelectrochemical techniques for the local investigation of corrosion procedures on solid surfaces, something which is not feasible with conventional large-scale techniques. In a second experiment the micro-electrochemical behavior of a faulty copper layer on 304L stainless steel was investigated using linear sweep voltammetry. Glass capillaries touching only small areas of the surface were used and the copper coated surface of the steel sample was scanned in a 9 by 6 matrix (54 measurements) while acquiring data. The obtained corrosion potentials for both defect and intact areas were used to map the surface. The surface plot shows the exact position of the defect point in the coating layer.

Keywords:

Microelectrochemistry, microcapillary, droplet cell, corrosion, stainless steel

¹ ISE member

1. Introduction

Capillary-based microcells are powerful tools for electrochemical surface investigations in the micrometer range. They can be used in the complete range of common electrochemical techniques, such as potential measurements, potentiostatic control in a three-electrode configuration, transient techniques including pulse and sweep techniques, and impedance spectroscopy.

Key differences between micro and macro scale systems confirm the high ability of microelectrodes in electroanalytical applications and also in kinetic studies [1-6]. Increasing the mass transport in micro systems is one of the most important differences between the two systems. By decreasing the surface area in micro systems the double layer capacitance is reduced and also micro systems obviously decrease the magnitude of the current passed [7] whereby small currents in the range of a few nA to some pA can be measured. Moreover, by applying different modifications to microcells, the evaluation and monitoring of additional parameters, such as pH, temperature, mechanical stress and electrolyte flow becomes possible [8].

A typical microcapillary cell is based on a standard three-electrode system containing a capillary in the range of $\leq 1000 \mu\text{m}$, which touches only a small area of a solid surface. In this setup the working electrode is the wetted area under the capillary tip. Therefore, measurements can be performed on selected micro areas of the sample. Different cell designs and capillary preparation methods have been discussed in the literature [9], along with various types of applications, including amongst other the microelectrochemical behavior of copper, 316L steel and aluminum, the investigation of aluminum-steel friction welds and a comparison of local electrochemical impedance spectroscopy of bi-electrodes and microcapillary cells [10-16].

In spite of the advantages, such as the study of microscopic surface areas and the direct evaluation of the initiation mechanism of localized corrosion [8], microcapillary techniques have some serious drawbacks, which sometimes makes their applications difficult [13]. Some of the most

important limitations which have been considered in previous works are: the resolution of the potentiostat, the Ohmic resistance specially in solutions with low conductivity and low concentrations, leakage and blockage of the capillary with oxidation or reduction products, such as oxygen and protons, and finally making capillaries with suitable tips for different aims (single measurement - surface scanning, etc.) [13,17-18]. The last mentioned limitation must be seriously considered when it comes to non-flat solid surfaces.

The objective of this work was to study the ability of a microcapillary electrochemical technique in the surface investigation of coated and bare 304L stainless steel and more specifically to make a comparison between localized and conventional large-scale surface analyses using voltammetric methods and electrochemical impedance spectroscopy. The first part of the work consists of the corrosion study of a bare 304L stainless steel sample in a sodium chloride solution in micro scale and so-called conventional large scale cells. The second part of the work focuses on the surface mapping of the 304L sample under a faulty copper coating.

2. Experimental

2.1. Specimens and surface preparation

Both localized and large scale measurements were performed on 304L stainless steel with the following chemical composition (wt. %): Cr: 17.65, Ni: 8.59, Mn: 1.75, Si: 0.41, C: 0.017, P: 0.032 and S: 0.005. The steel samples (coupons with a diameter of 12.5 mm and thickness of 2 mm) were mechanically grounded with silicon carbide paper down to 600 grit and then polished with alumina powder ($< 0.5 \mu\text{m}$), washed with distilled water and then rinsed ultrasonically in ethanol for 5 minutes.

For the second experiment, a thin copper layer was electrodeposited on a 304L stainless steel plate (2×3 cm). The latter was done according to the electrodeposition method described by Pardo et al.

[19]. In brief the polished stainless steel plate was pickled in a mixture of HNO₃ 15 wt.% and HF 2 wt.% at 60 °C for 2 minutes. The electrodeposition itself was performed in a saturated H₂SO₄/CuSO₄·5H₂O solution using a potentiometric (galvanostatic) method with a current density of ~ 0.08 A and a duration time of 300 s. A small defect point (~ 300 μm) was made in the center of the copper layer using a micro needle.

2.2. Preparation of the sealed microcapillary

The microcapillaries were obtained by heating glass Pasteur pipettes (2 mL) until the glass melting point and then pulling them in a special manner. The tip surface of the prepared capillaries were polished using first 600 and then 1200 grit silicon carbide (SiC) papers. This way tip diameters of 100 μm (first set of experiments) and 600 μm (second set of experiments) were obtained. In order to prevent leaking of the electrolyte, a silicon gasket was attached to the capillary tip. The latter was prepared by dipping the capillaries into silicon rubber, after which a stream of nitrogen was flushed through the microcapillary to keep the tip of the capillaries open without destroying the gasket. An optical microscope was used to monitor the procedure. By repeating this procedure for 2 or 3 times, thin layers of silicon were applied onto the tip of the capillaries (Figure 1). Depending on the type of the surface analysis, the sealed microcapillary can be attached to the solid surface before drying for a single measurement or can be used after drying for surface scanning.

2.3. Electrochemical set-up

The localized micro-electrochemical measurements were performed using a homemade microcapillary cell (Figure 2) attached to an Autolab Eco Chemie potentiostat (PGSTAT 10). The setup is based on a common three-electrode system containing a thin platinum wire as counter

electrode, a saturated Ag/AgCl reference electrode and a sealed microcapillary with a silicon gasket and with ground tip diameter of 600/100 μm which touches only a small part of the solid sample placed on a platinum plate and forms the working electrode. The platinum plate itself is attached to a fiberglass plate with a number of holes and plastic screws, which makes it possible to fix different samples with different sizes on it before measurement (not shown in Figure 2). To minimize the Ohmic resistance during the measurement the counter electrode (here platinum wire) was placed near the tip of the microcapillary.

The large-scale electrochemical measurements were performed using the same potentiostat in a three-electrode cell with a saturated Ag/AgCl/KCl reference electrode and a platinum plate as auxiliary electrode.

Both localized and large scale electrochemical impedance measurements (EIS) were performed in a 1 M NaCl solution using a frequency range of 20 KHz to 0.01 Hz. An amplitude of 50 mV at open circuit potential was used to decrease the noise and obtain smooth graphs. Nyquist plots of the sample were recorded before and after potentiodynamic polarization of the wetted surface. The latter was performed using linear sweep voltammetry. The potential range was between -1.5 and 1.3 V (vs. Ag/AgCl) for the both micro and large scale techniques.

In the localized surface mapping of the second experiment, the microcapillary was scanned in a 9 by 6 matrix (54 measurements) across the surface while acquiring data for voltammetric technique (Figure 3). For this the sample surface was divided into little squares of ca 2×2 mm using a marker, which allowed us to position the microcapillary for each measurement. The scanning was done by moving the sample. At each point a voltammetric scan in the potential range of -1.5 till 1.3 V (vs. Ag/AgCl) were performed. The obtained Tafel plots were used to calculate the corrosion potential (E_{corr}) for each measured point.

Scanning electron images of the surface were taken using a Phenom-FEI electron microscope.

3. Results and Discussion

3.1. Comparison of localized and conventional electrochemical measurements

Figure 4 shows the Tafel plots of the stainless steel sample after each polarization obtained by the local and the conventional experiments. Both local and large scale potentiodynamic polarizations were performed on one specific spot of the sample. The localized Tafel plots show that the corrosion potential of the steel shifts from -580 mV (1st polarization) towards more negative potentials after each polarization. Finally after the 6th polarization the plot shows a corrosion potential with a value of about -735 mV. A similar potential shift was observed for the large scale polarization experiment. In this case the corrosion potential of the steel disc shifts from -986 mV (1st polarization) to -1014 mV after the third polarization. In both localized and conventional large scale polarizations the first scan is performed on the bare steel surface coated by a passive oxide film. Therefore, the next polarizations remove this passive layer and the corrosion potential continuously decreases especially on the micro scale.

Figure 4 also shows that the corrosion process of steel on a micro scale occurs at more positive potentials compared to the macroscopic scale. Similar results have been reported by Böhni in the case of pitting potentials of stainless steel measured by microelectrodes with different diameters from 50 μm till 1000 μm (large scale) where the pitting potentials of steel decreases with increasing surface area [20]. According to Schultze [21], the charge transfer reactions and also the transport and reaction mechanisms in solution in both micro and macro systems are the same. In spite of this, some differences appear when the applied potential or current focuses on a micro point. In the other words, the kinetics of microelectrochemical reactions strongly depend on the size of the electrode. More specifically, the difference arises when a random phenomena such as pit formation becomes dominant [21-22]. Therefore, the difference in the corrosion potentials and also in the corrosion currents, which in micro scale measurements is clearly lower than in

conventional systems, can be concluded as the results of the decrease in the exposed surface area in micro systems.

The difference between macro and micro electrochemical behavior of stainless steel is observed also in the EIS analyses, where the pit formation on the wetted surface under the microcapillary after the potentiodynamic polarization shows a direct effect on the local electrochemical impedance spectroscopy of the sample. In fact, localization of the solid surface under the microcapillary achieves more detailed results by limitation of the diffusion layer in solid/liquid interface [21]. The Nyquist diagrams of the large scale and micro scale measurements are shown in Figures 5 and 6 respectively. It is seen that in the large scale measurements the real impedance (Z') against the imaginary impedance ($-Z''$) of steel increases with a more or less constant slope before and after 3 polarization cycles of the immersed surface in the entire frequency range (Figure 5). The spectra are fitted with the theoretical Nyquist plot for Warburg impedance which represents the diffusion of ionic species at the electrode/electrolyte interface [23]. In this figure the slope of the Nyquist spectrum decreases after the first and second polarizations while after the third polarization the value of the real impedance against the imaginary impedance increases.

For the micro scale measurements the Nyquist diagrams of the wetted spot of the steel sample under a 100 μm microcapillary clearly show the corrosion procedure of steel in NaCl solution (Figure 6). In this case, the local spectrum before the polarization is characterized by a depressed semicircle, which is removed after the first polarization together with the first decrease in the corrosion potential (Figure 4). After the 2nd polarization the initiation of a new semicircle is observed, which grows after the 3rd polarization. The peak area of the semicircle spectrum appears in the frequencies around 7.4 KHz ($-Z''$: $\sim 0.35 \text{ M}\Omega$). After the 4th polarization both imaginary and real impedance values increase. Here the peak area appears at frequencies around 2.8 KHz with relative imaginary impedance of almost 1 $\text{M}\Omega$. After the 5th polarization decreases the peak imaginary impedance decreases again to value to less than 0.4 $\text{M}\Omega$. Finally after the 6th polarization, the imaginary impedance grows against the real impedance till $\sim 0.6 \text{ M}\Omega$ in the peak

area in frequency of ~ 6 KHz. Based on these results, it can be concluded that the first polarization of the wetted area of the sample removes the passive film on the surface while after the next polarizations a corroded layer forms under the microcapillary and therefore shifts the corrosion potential of steel toward more negative potentials (see above). A SEM image of the corroded point of the steel sample after 6 potentiodynamic polarizations is shown in Figure 7.

A description of the localized impedance diagram before and after the polarizations cycles using an equivalent circuit presented in Figure 8. Here R_{Ω} is the Ohmic resistance which depends on the conductivity of the electrolyte and the geometry of the electrode; C_{dl} represents the double layer capacitance which is an electrical double layer at the electrode/electrolyte interface; R_{ct} shows the charge transfer resistance which depends on the conductivity of the electrolyte; Z_{war} is the Warburg impedance which represents the diffusion of ionic species at the electrode/electrolyte interface; R_p is polarization resistance which means the potential of the electrode forced away from its value at open circuit and C_p is capacitance. The local impedance spectra of the steel sample in NaCl solution before and after the 2nd potentiodynamic polarization can be simulated with circuit (a) in Figure 8. This model usually can be used for example to describe the impedance of a coating layer (here passive film on the steel surface) on a metal substrate in contact with an electrolyte [23-25]. The Nyquist plot after the first polarization shows a Warburg impedance (Z_{war}) which appears as a straight line with a slope of 45° . The circuit (b) of Figure 8 can be considered for the Nyquist spectrums after the 3rd – 6th polarizations which show semicircles with a 45° tail after them in lower frequencies. This model normally is used when both kinetics and diffusion are important [23-25]. Here the model consists of a double layer capacitance which is not observed in the first model. In contrast the first model consists of an additional capacitance and Ohmic resistance in the circuit. In brief, the corrosion investigation of a solid surface in macro and micro scales can show completely different procedures.

3.2. Surface map of the 304L stainless steel sample with deposited copper layer

The obtained surface map of the corrosion potential around the defect point is shown in Figure 9. It shows that the observed corrosion potential at the defect area of the coating drops to -600 mV, while the measured corrosion potential on the intact area of the copper layer is around -300 mV. This surface map confirms that when a coating contains small pinholes, such as the defect of 300 μm in this work, the corrosion of steel can initiate from the weak area with more negative corrosion potential.

4. Conclusions

A comparison of the localized and conventional large-scale impedance measurements on a 304L stainless steel sample has shown that local EIS measurements provide essential information to characterize the local corrosion procedure, while the conventional large-scale systems are not able to follow the detailed corrosion procedure on the solid surfaces. In addition, surface scanning solid samples with a microcapillary enable us to describe the detailed properties of an electroactive solid surfaces.

Acknowledgements

UGent (BOF) is acknowledged for funding this work.

References

- [1] M. Fleischmann, F. Lasserre, J. Robinson, D. Swan, J. Electroanal. Chem. 117 (1984) 97.
- [2] J. Galceran, J. Puy, J. Salvador, J. Cecilia, H. P. Van Leeuwen, J. Electroanal. Chem. 505 (2001) 85.
- [3] B.A. Brookes, G. Macfie, R. G. Compton, J. Phys. Chem. B. 104 (2000) 5784.

- [4] H.P. Van Leeuwen, J. P. Pinheiro, *J. Electroanal. Chem.* 471 (1999) 55.
- [5] A. Molina, C. Serna, F. Martinez-Ortiz, *J. Electroanal. Chem.* 486 (2000) 9.
- [6] S. Komrosky-Lovric, M. Lovric, A. Bond, *Electroanal.* 5 (1999) 29.
- [7] N.V. Rees, R. G. Compton, *Russ. J. Electrochem.* 44 (2006) 369.
- [8] T. Suter, H. Böhni, *Electrochim. Acta* 47 (2001) 191.
- [9] M.M. Lohrengel, *Corros. Eng. Sci. Techn.* 39(1) (2004) 55.
- [10] M. Sanchez, J. Gamby, H. Perrot, D. Rose, V. Vivier, *Electrochem. Commun.* 12 (2010) 1230.
- [11] M. Schindler, U. Langklotz, A. Michaelis, B. Arnold, *Surf. Interface Anal.* 42 (2009) 281.
- [12] J. Jorcin, H. Krawiec, N. Pebere, V. Vignal, *Electrochim. Acta* 54 (2009) 5775.
- [13] H. Krawiec, V. Vignal, R. Akid, *Electrochim Acta* 53 (2008) 5252.
- [14] C. Dong, A. Fu, X. Li, Y. Cheng *Electrochim. Acta* 54 (2008) 628.
- [15] F. Andreatta, M. Lohrengel, H. Terryn, J. Wit, *Electrochim. Acta* 48 (2003) 3239.
- [16] T. Hamelmann, M. Lohrengel, *Electrochim. Acta* 47 (2001) 117.
- [17] N. Birbilis, B.N. Padgett, R.G. Buchheit, *Electrochim. Acta* 50 (2005) 3536.
- [18] F. Andreatta, M.M. Lohrengel, H. Terryn, J.H.W. de Wit, *Electrochim. Acta* (2003) 48, 3239.
- [19] A. Pardo, M.C. Merino, A.E. Coy, R. Arrabal, F. Viejo, A. M'hich, *Appl. Surf. Sci.* 253(23) (2007) 9165.
- [20] H. Böhni, T. Suter, A. Schreyer, *Electrochim. Acta* 40 (1995) 1367.
- [21] J.W. Schultze, A. Bressel, *Electrochim. Acta* 47 (2001) 7.
- [22] J.W. Schultze, V. Tsakova, *Electrochim. Acta* 44 (1999) 3610.
- [23] P.L. Bonora, F. Deflorian, L.Fedrizzi, *Electrochim. Acta* 41 (1996) 1074.
- [24] C. Ruan, L. Yang, Y. Li, *Anal. Chem.* 74 (2002) 4818.
- [25] C. Liu, Q. Bi, A. Leyland, A. Matthews, *Corros. Sci.* 45 (2003) 1254.

Figure captions

- Figure 1. Optical image of a microcapillary with silicon gasket.
- Figure 2. Schematic drawing of the set-up of the capillary-based droplet cell.
- Figure 3. Scheme of surface mapping with a microcapillary electrochemical droplet cell.
- Figure 4. Tafel plots of the 304L stainless steel sample in a 1 M NaCl solution. Above: large-scale, after 3 polarizations (scan rate: 10 mV/s). Below: localized by a microcapillary with a tip diameter of 100 μm (6 polarizations).
- Figure 5. Nyquist diagrams of a 304L stainless steel coupon measured in a 1 M NaCl solution before and after each potentiodynamic polarization.
- Figure 6. Nyquist diagrams of a 304L stainless steel sample measured locally in a 1 M NaCl solution using a microcapillary with a tip diameter of 100 μm before and after each potentiodynamic polarization.
- Figure 7. Scanning electron image of the 304L stainless steel sample after 6 localized polarizations by a microcapillary with a tip diameter of 100 μm using linear sweep voltammetry in a 1 M NaCl solution. Scan rate: 10 mV/s.
- Figure 8. Electrical equivalent circuit of the corroded layer under a microcapillary before and after the 2nd (a) and after the 3rd – 6th (b) potentiodynamic polarization of the wetted surface.
- Figure 9. Localized voltammetric map of a copper coated 304L stainless steel plate around a defect area of $\sim 300 \mu\text{m}$ in diameter by a microcapillary with a tip diameter of 600 μm using linear sweep voltammetry (scan rate: 10 mV/s).

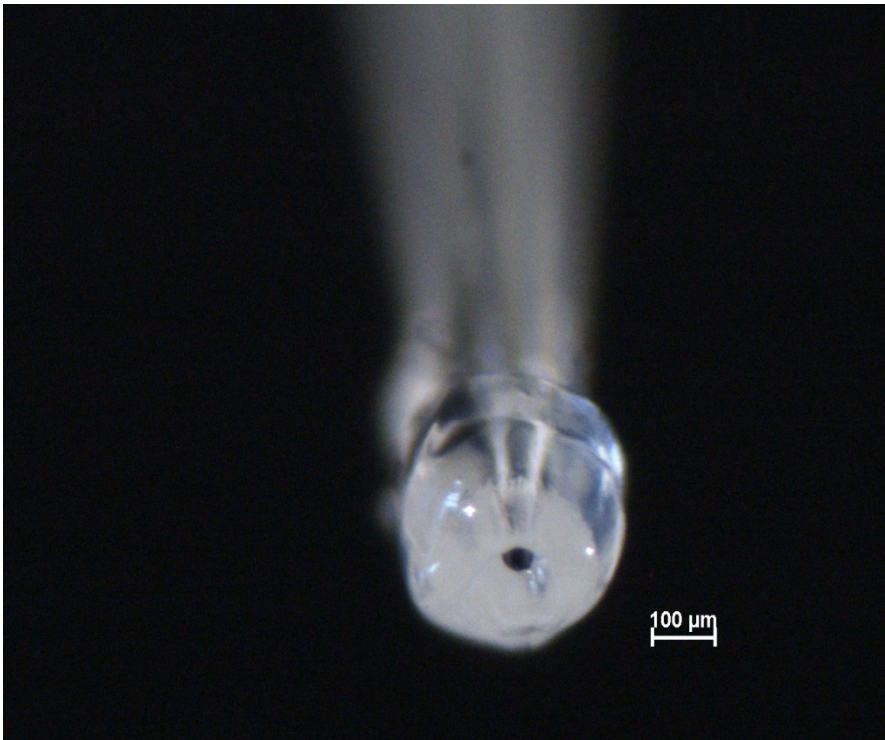


Fig. 1.

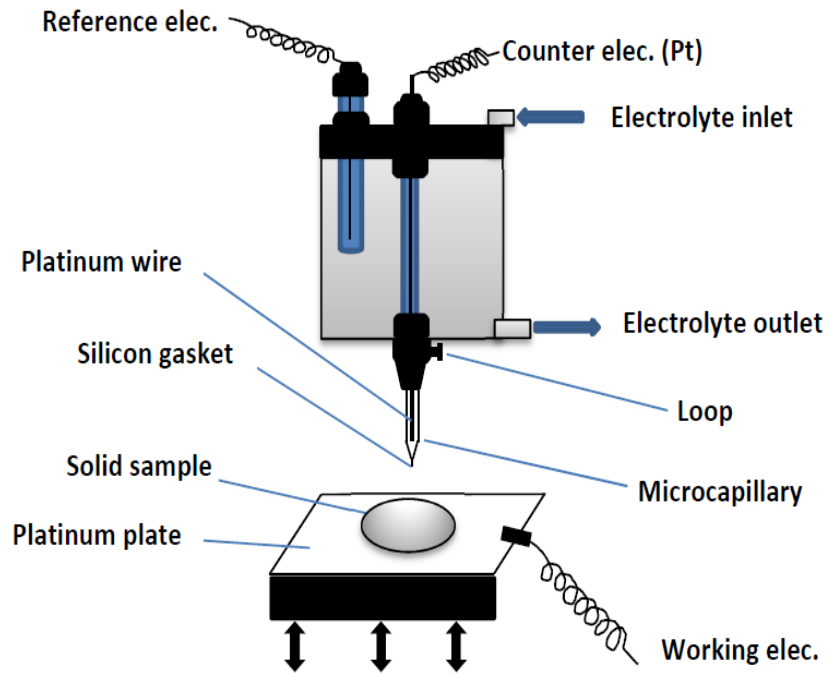


Fig. 2.

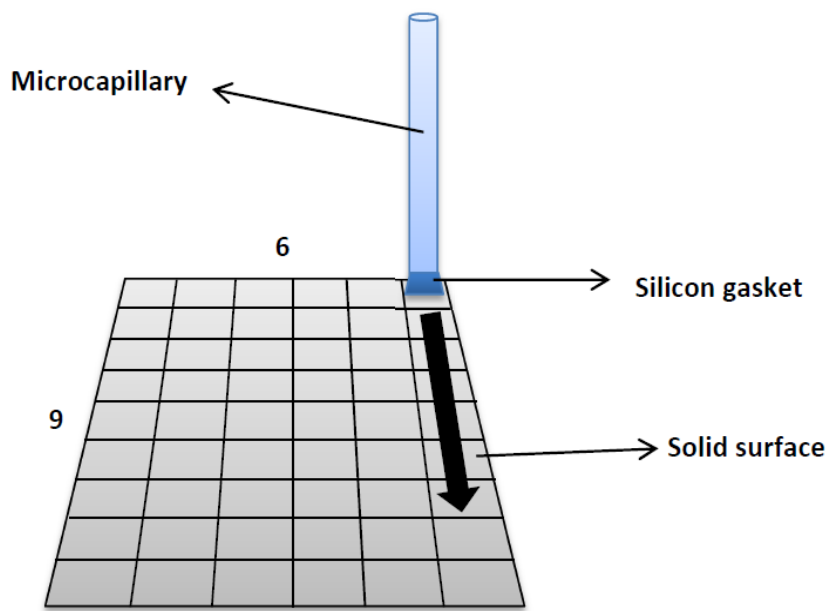


Fig. 3.

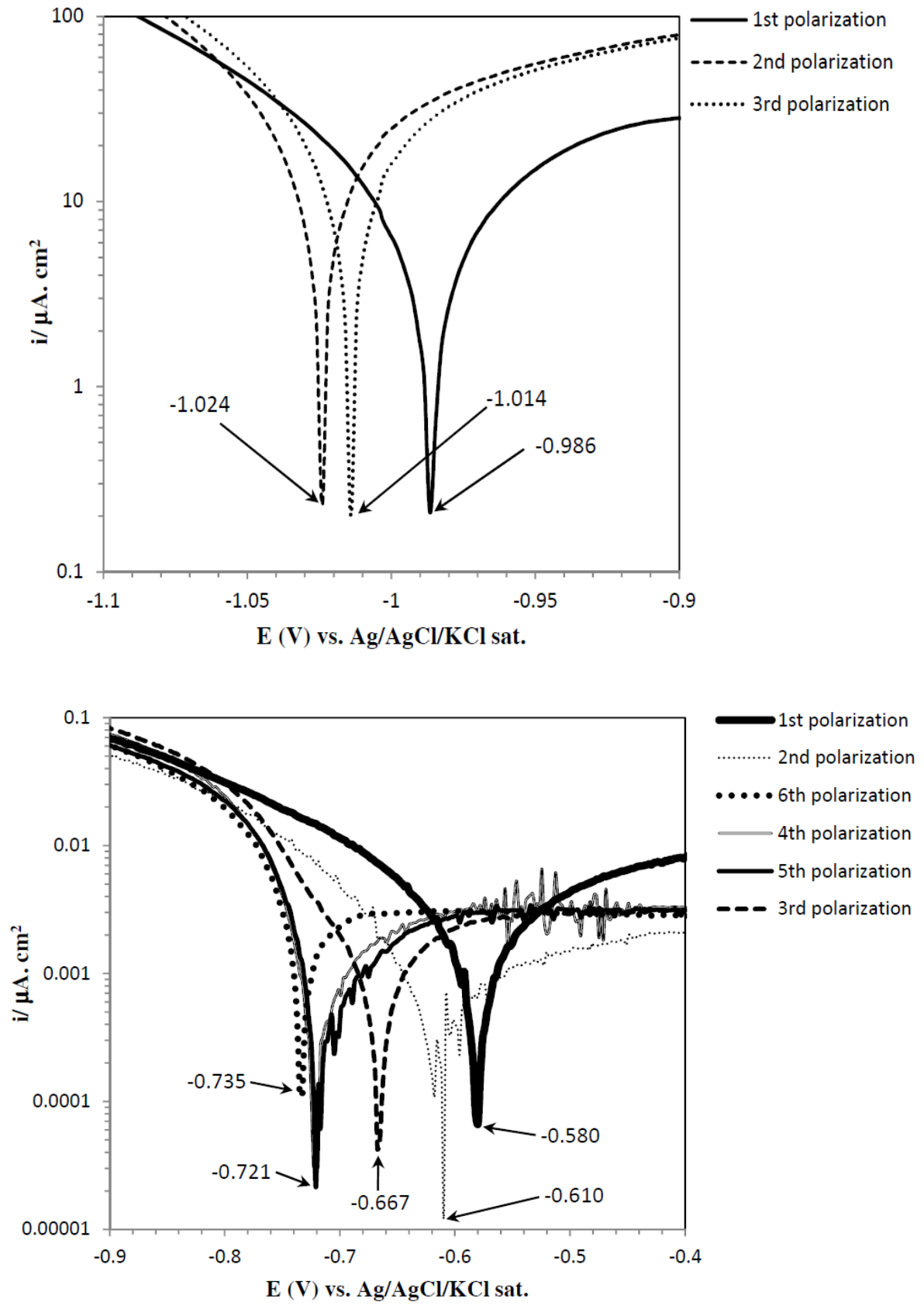


Fig. 4.

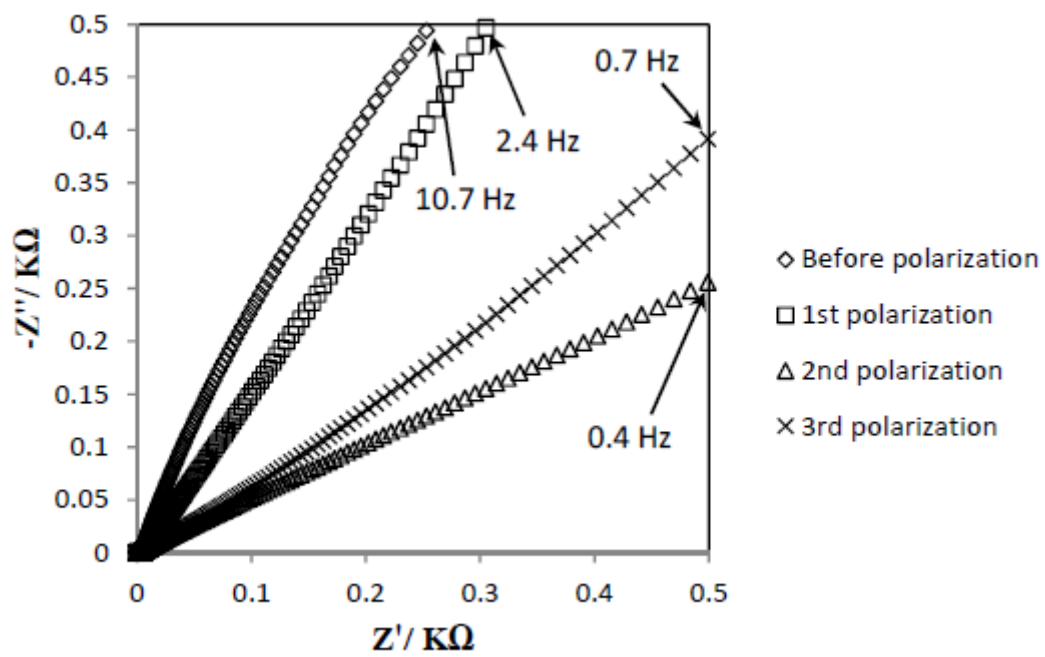
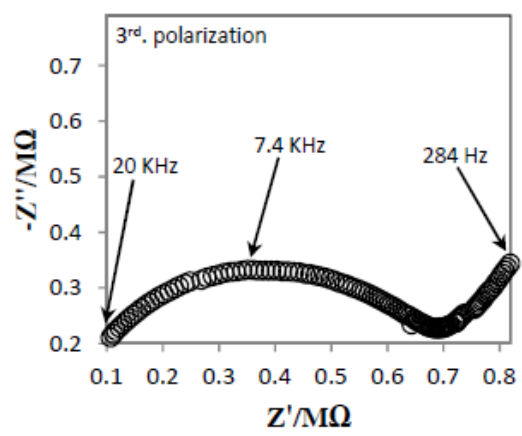
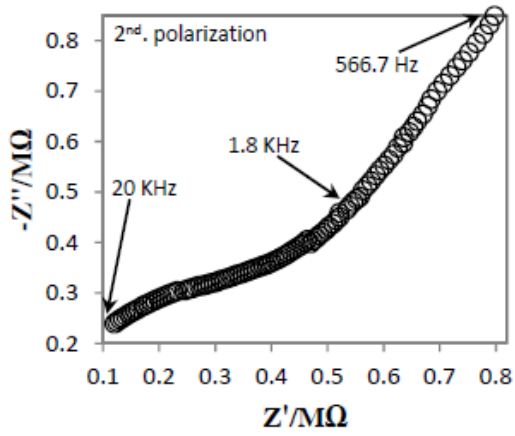
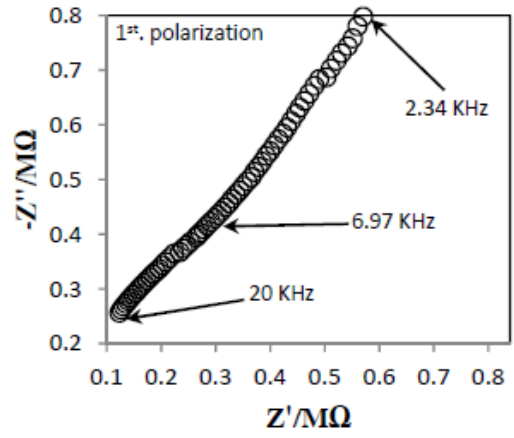
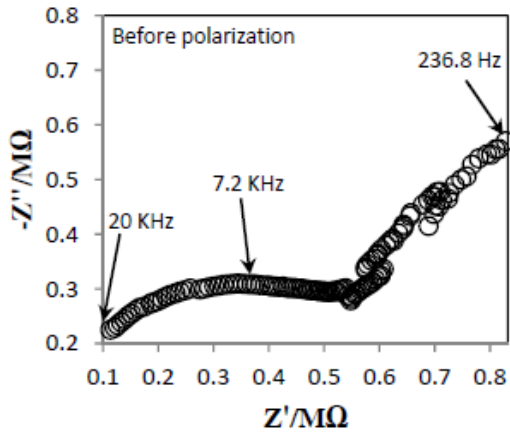


Fig. 5.



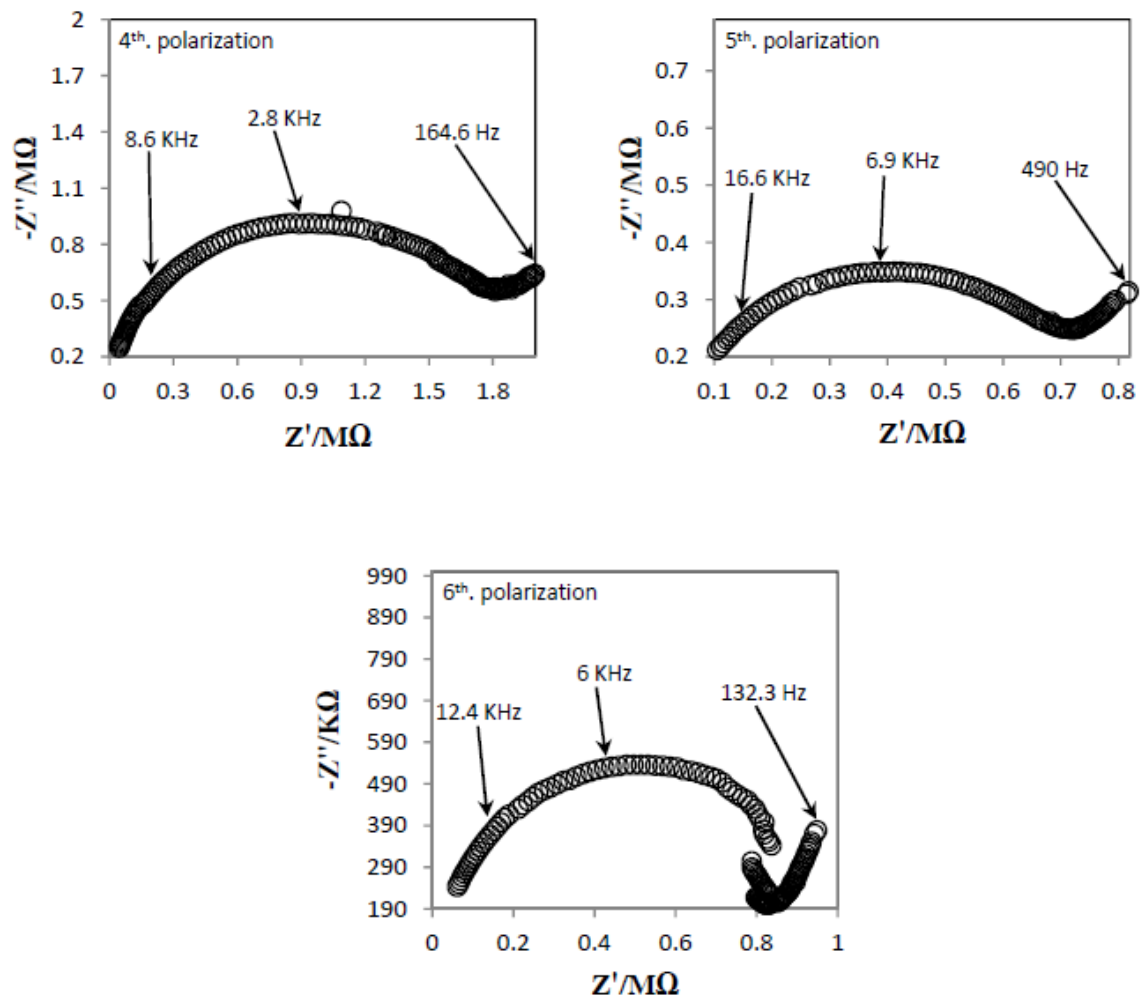


Fig. 6.

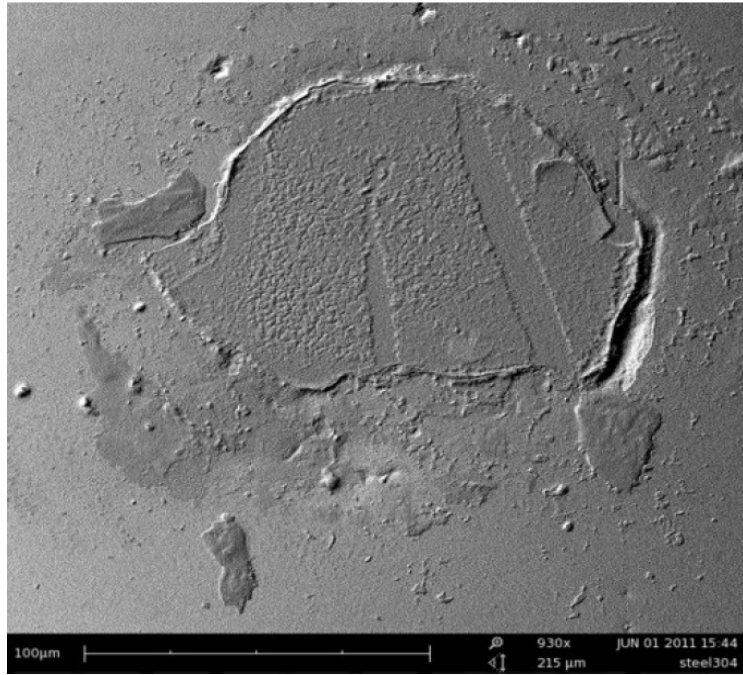


Fig. 7.

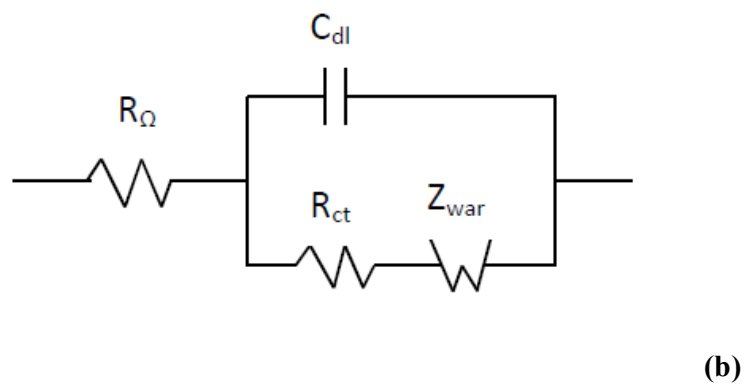
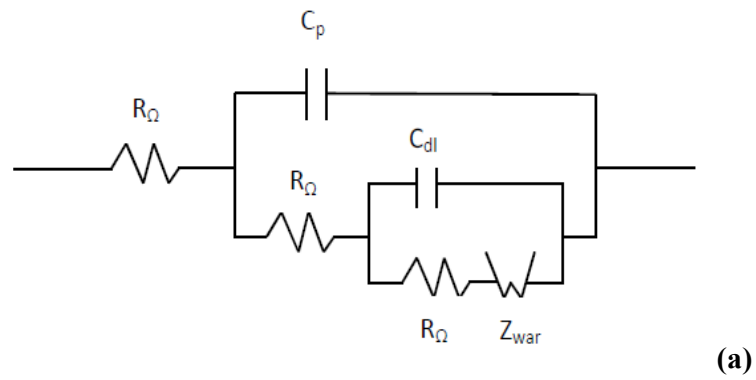


Fig. 8.

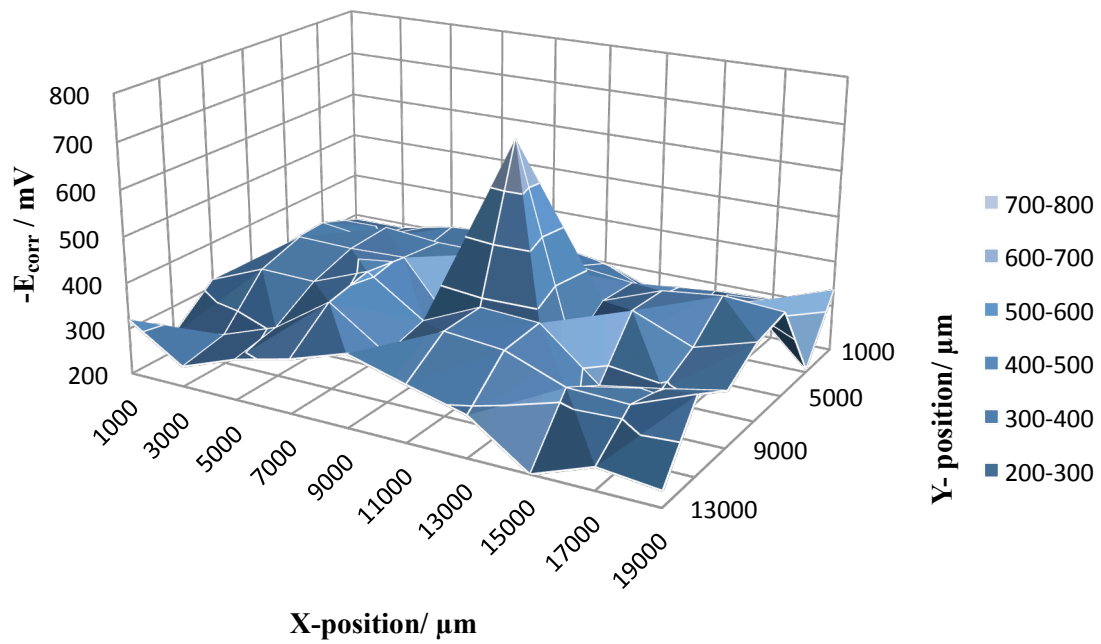


Fig. 9.